Morphogenesis checkpoint kinase Swe1 is the executor of lipolysis-dependent cell-cycle progression

Neha Chauhan, Myriam Visram, Alvaro Cristobal-Sarramian, Florian Sarkleti, and Sepp D. Kohlwein[1]

Institute of Molecular Biosciences, BioTechMed Graz, University of Graz, A8010 Graz, Austria

Edited by Daniel E. Gottschling, Fred Hutchinson Cancer Research Center, Seattle, WA, and approved February 2, 2015 (received for review December 10, 2014)

Cell growth and division requires the precise duplication of cellular DNA content but also of membranes and organelles. Knowledge about the cell-cycle–dependent regulation of membrane and storage lipid homeostasis is only rudimentary. Previous work from our laboratory has shown that the breakdown of triacylglycerols (TGs) is regulated in a cell-cycle–dependent manner, by activation of the Tgl4 lipase by the major cyclin-dependent kinase Cdc28. The lipases Tgl3 and Tgl4 are required for efficient cell-cycle progression during the G1/S (Gap1/replication phase) transition, at the onset of bud formation, and their absence leads to a cell-cycle delay. We now show that defective lipolysis activates the Swe1 morphogenesis checkpoint kinase that halts cell-cycle progression by phosphorylation of Cdc28 at tyrosine residue 19. Saturated long-chain fatty acids and phytosphingosine supplementation rescue the cell-cycle delay in the Tgl3/Tgl4 lipase-deficient strain, suggesting that Swe1 activity responds to imbalanced sphingolipid metabolism, in the absence of TG degradation. We propose a model by which TG-derived sphingolipids are required to activate the protein phosphatase 2A ($PP2A^{Cdc55}$) to attenuate Swe1 phosphorylation and its inhibitory effect on Cdc28 at the G1/S transition of the cell cycle.

triglyceride | lipase | G1/S transition | cyclin-dependent kinase | sphingolipid

The eukaryotic cell cycle is a highly coordinated and conserved process. In addition to DNA replication, one of the major requirements for the cell to progress through the cell cycle is the precise duplication of membrane-enclosed organelles and other cellular components before cell division. Knowledge about the mechanisms regulating (membrane) lipid homeostasis during the cell cycle is scarce (1), however several levels of evidence suggest regulation of key enzymes of lipid metabolism in a cell-cycle–dependent manner. The *PAH1*-encoded phosphatidic acid (PA) phosphatase (Pah1), a key enzyme of triacylglycerol (TG) synthesis that provides the TG precursor diacylglycerol (DG), is phosphorylated and inactivated by the cyclin-dependent kinases Cdc28 and Pho85–Pho80 (2, 3). Kurat et al. showed that Tgl4, next to Tgl3, one of the two major TG lipases in yeast and the ortholog of mammalian ATGL (4, 5), is also phosphorylated by Cdc28. In contrast to Pah1, however, Tgl4 is activated by Cdc28 (6). This inverse regulation of Pah1 and Tgl4 by Cdc28-dependent phosphorylation led to the model by which the TG content oscillates during the cell cycle: On the one hand, TG synthesis serves as a buffer for excess de novo generated fatty acids (FAs), and on the other hand, in times of increased demand—that is, at the onset of bud formation and bud growth—Tgl4-catalyzed lipolysis becomes active to provide TG-derived precursors for membrane lipid synthesis (6).

TG and membrane phospholipids share the same intermediates, PA and DG; PA is generated by sequential acylation of glycerol-3-phosphate, reactions that mostly take place in the endoplasmic reticulum (ER) membrane (7). The dephosphorylation of PA to DG by the *PAH1*-encoded PA phosphatase Pah1 is the major regulator of cellular TG synthesis in yeast (8), similar to its mammalian ortholog, lipin (9). According to this central role, TG content in *PAH1*-deficient yeast cells is decreased by 70–90%; the source of the residual TG in these mutants is currently unclear. TG synthesis from DG requires one additional acylation step that is catalyzed by the *DGA1*-encoded acyl-CoA–dependent DG acyltransferase (10, 11) and the phospholipid-dependent acyltransferase, encoded by *LRO1* (7). Alternatively, in the presence of the phospholipid precursors, ethanolamine and/or choline, DG may be converted into phospholipids via the Kennedy pathway (7). Thus, net TG synthesis in growing cells is determined by multiple factors, including the availability of FAs, presence of lipid precursors, and the activities of PA phosphatase and the DG acyltransferases. Degradation of TG in yeast is governed by the major lipid droplet (LD)-associated lipases, encoded by *TGL3* and *TGL4* (4, 12); both enzymes belong to the patatin-domain–containing family of proteins, members of which play a crucial role in lipid homeostasis also in mammals (13). Multiple additional lipases exist in yeast, but their specific function and contribution to TG homeostasis may be restricted to specific growth conditions (7, 14, 15).

Absence of lipolysis in mutants lacking *TGL3* and *TGL4* results in up to threefold elevated levels of TG and reduced levels of phosphatidylcholine and sphingolipids (4, 12, 16, 17), indicating that TG breakdown provides precursors for these lipids or generates some regulatory factors required for their synthesis. The rate of phosphatidylinositol (PI) synthesis after readdition of inositol to inositol-starved cells is reduced by 50% in lipase-deficient cells; the boost of PI synthesis under inositol refeeding conditions is completely abolished if de novo FA synthesis is additionally blocked in the lipase mutants by the inhibitor cerulenin (18). These data clearly demonstrate the requirements for TG breakdown, in addition to de

Significance

Little information is currently available on how a cell coordinates the expansion of its membranes with growth and cell-cycle progression. Synthesis (lipogenesis) and degradation (lipolysis) of the major storage lipid triacylglycerol (TG) are regulated in yeast by the cyclin-dependent kinase Cdc28. TG breakdown provides precursors for the synthesis of sphingolipids, which in turn regulate cell-cycle progression upon exit from G0 phase of the cell cycle via the regulatory circuit comprised of Cdc55 phosphatase, Swe1 morphogenesis checkpoint kinase, and Cdc28 cyclin-dependent kinase. This finding unveils an unexpected function of the Swe1 morphogenesis checkpoint kinase in regulating lipolysis-dependent cell-cycle entry from G0.

Author contributions: N.C. and S.D.K. designed research; N.C., M.V., A.C.-S., and F.S. performed research; F.S. contributed new reagents/analytic tools; N.C., M.V., A.C.-S., and S.D.K. analyzed data; and N.C. and S.D.K. wrote the paper.

The authors declare no conflict of interest.

This article is a PNAS Direct Submission.

Freely available online through the PNAS open access option.

[1]To whom correspondence should be addressed. Email: sepp.kohlwein@uni-graz.at.

This article contains supporting information online at www.pnas.org/lookup/suppl/doi:10.1073/pnas.1423175112/-/DCSupplemental.

novo FA synthesis, to generate precursors for membrane lipids. As a consequence of defective lipolysis, entry of quiescent cells into vegetative growth is significantly delayed; thus, TG breakdown is particularly important for promoting exit from the stationary phase and entry into the gap1 (G1) phase of the cell cycle (4, 6, 19).

Progression through the cell cycle is regulated by specific checkpoint pathways that ensure completion of crucial events and execute a halt under nonconducive conditions. Checkpoint mechanisms slow down or arrest the cell cycle to enable cells to fix damage or to obtain the required metabolites before proceeding and are as such important for the integrity of cell division (20–22). According to this critical function in quality control, mutations in checkpoint genes in mammals have been linked to cancer predisposition and progression. The first discovered cell-cycle checkpoint in *Schizosaccharomyces pombe* that regulates entry into mitosis is executed by the Wee1 kinase (23, 24), which delays mitosis by phosphorylating and inhibiting cyclin-dependent kinase Cdk1 (25). Conversely, the phosphatase Cdc25 promotes entry into mitosis by removing the inhibitory phosphorylation of Cdk1 (26–28). The budding yeast orthologs of Wee1 and Cdc25 are called Swe1 and Mih1, and their key functions in regulating Cdk1 activity are highly conserved (29, 30). Swe1 phosphorylates Cdk1 (encoded by *CDC28* in budding yeast) at the tyrosine 19 residue and inhibits its kinase activity (29, 31, 32); the Mih1 phosphatase removes this inhibitory phosphorylation initiating G2/M cell-cycle progression (26). The Swe1 and Cdk1/Cdc28 kinases operate in an autoregulatory loop in which Swe1 is initially phosphorylated and activated by Cdk1/Cdc28 that is associated with mitotic cyclins; subsequently, activated Swe1 phosphorylates and inhibits Cdk1/Cdc28 (33). The initial phosphorylation of Swe1 is opposed by the protein phosphatase 2A (PP2A) with its catalytic subunits Pph21 or Pph22 and the regulatory subunit Cdc55 ($PP2A^{Cdc55}$), which sets a threshold, limiting the activation of Swe1 by Cdk1/Cdc28 in early mitosis (34, 35). Loss of the regulatory subunit Cdc55 leads to hyperactivation of Swe1 (35); after the initial phosphorylation of Swe1 in early mitosis, subsequent phosphorylation events trigger full hyperphosphorylation of Swe1 (33), which leads to its ubiquitin-mediated degradation (36, 37). Of note, regulation of Cdk1/Cdc28 by the G1 cyclin Cln2 plays an important role in actin cytoskeleton polarization and the localized delivery of secretory vesicles, which contribute membrane lipids to the developing bud, thus linking cell surface growth to the cell cycle (38).

Despite its proposed role as a gap2 phase (G2) checkpoint regulator, we now show that Swe1 kinase is responsible for the G1/S (Gap1/replication phase) cell-cycle delay in mutants defective in TG lipolysis by phosphorylating Cdk1/Cdc28 at tyrosine 19. Deletion of Swe1 in the *tgl3 tgl4* lipase mutant restores normal cell-cycle progression; similarly, supplementation of mutant cells with saturated FAs (myristic acid, palmitic acid) or a precursor of sphingolipid synthesis, phytosphingosine (PHS), suppress the cell-cycle delay in the lipase mutants. These data suggest that Swe1 is a lipid-regulated kinase that is activated in the absence of specific lipids, presumably sphingolipids, and halts G1/S transition by phosphorylating Cdk1/Cdc28 in lipase-deficient cells that exit from the G0 phase of the cell cycle.

Results and Discussion

Tgl3/Tgl4-Catalyzed Lipolysis Provides Precursors to Promote G1/S Cell-Cycle Progression. Previous work from our laboratory has demonstrated a requirement of lipolysis for efficient cell-cycle progression (6). Absence of the major TG lipases Tgl3 and Tgl4 extends the G1/S transition of the cell cycle by ~30 min in RediGrad-synchronized G0 cells (Fig. 1*A*). This cell-cycle delay is also reflected in the timing of the onset of bud formation (Fig. 1*B*), consistent with previous results (6). However, there was no general defect in cell growth during the log phase, and all mutants essentially reached the same cell density in the stationary phase (Fig. S1). Because the primary products of lipolysis are FAs, we next investigated whether their external administration would suppress the cell-cycle delay of *tgl3 tgl4* mutants. This was indeed the case when either myristic acid (C14:0) or palmitic acid (C16:0) were supplied (Fig. 1 *A* and *B*), whereas unsaturated FAs (C16:1 or C18:1) did not suppress the cell-cycle delay. This result is surprising, as C16:1 and C18:1 represent the major FA species in yeast (~80% of total FA content), and further suggests a physiological requirement for specific FAs rather than their use as potential energy substrates. Because cells are maintained in media containing glucose, β-oxidation, which in yeast only takes place in peroxisomes, is typically repressed (15). Mutants lacking key enzymes of β-oxidation, Pox1 and Pox3/Pot1, indeed do not show a cell-cycle delay, further excluding the possibility that lipolysis provides FAs for energy production during the initiation of the cell cycle (Fig. S2).

The specific requirement for saturated FAs that may be precursors for sphingolipids prompted us to investigate whether long-chain base supplementation also rescued the cell-cycle delay in the lipase-deficient mutant. This was indeed the case (Fig. 1 *A* and *B*) and is consistent with previous observations that sphingolipid synthesis is impaired in *tgl3 tgl4* mutants (39). This impairment is also reflected in the slightly increased sensitivity of *tgl3 tgl4* mutants to the inhibitor myriocin, which blocks the first step in sphingoid long-chain base synthesis, serine palmitoyl

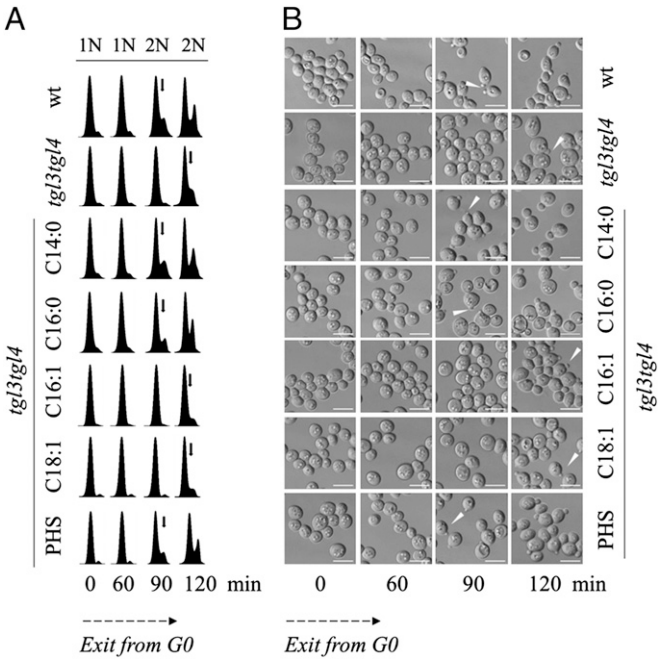

Fig. 1. Deletion of Tgl3 and Tgl4 results in a cell-cycle delay at G1/S. Cells were grown for 7 d in YPD medium, and quiescent (G0) cells were obtained by RediGrad centrifugation. After release into fresh glucose containing minimal media, cells were harvested at the indicated time points and analyzed by FACS and microscopy. (*A*) In the lipase-deficient *tgl3 tgl4* mutant, entry into the S phase is delayed. Wild type entered the cell cycle 90 min after release, and the 2N peak in *tgl3 tgl4* appears 30 min later, at 120 min. Supplementation of media with FAs, C14:0 and C16:0 (0.025% in 1% tergitol), or PHS (1 μM in 0.2% tergitol) rescues the cell-cycle delay of the *tgl3 tgl4* mutant: The 2N peak in the *tgl3 tgl4* mutant starts to appear 90 min after release, similar to wild type. The unsaturated FAs (C16:1 and C18:1) have no effect on cell-cycle progression of the *tgl3 tgl4* mutant. Initiation of the S phase is indicated by arrows. Experiments were performed in biological triplicates. (*B*) The timing of bud formation was analyzed in synchronized G0 cells by microscopy. Initiation of bud formation (indicated by white arrowheads) occurs concomitantly with the G1/S phase cell-cycle transition under all conditions tested. (Scale bar, 10 μm.)

transferase (SPT) (40). Supplementation with long-chain base PHS but not with palmitic acid fully rescues myriocin sensitivity, as expected (Fig. S1*C*). Taken together, the cell-cycle delay of the *tgl3 tgl4* mutant that is defective in TG degradation does not result from a general growth defect and is specific for the entry of quiescent G0 cells into a new cell cycle. Suppression of the delay by sphingolipid precursors suggests that Tgl3/Tgl4-catalyzed lipolysis provides precursors for these lipids.

Absence of Inositol Extends the G1/S Cell-Cycle Delay of the *tgl3 tgl4* Mutant. PI plays an essential role as a precursor for complex sphingolipids. Gaspar et al. previously showed that absence of lipolysis drastically attenuates the synthesis of PI upon administration of inositol to inositol-starved cells, suggesting that TG-derived metabolites provide precursors for PI production (18). In addition, we have previously reported that lack of inositol in standard cultivation media extends the cell cycle at the G2/M boundary (41), demonstrating that endogenous inositol production is limiting even in wild-type cells during logarithmic growth. Thus, we next investigated whether and to what extent inositol depletion affected cell-cycle progression in wild-type and lipase-deficient mutants (Fig. S3). RediGrad-synchronized G0 phase cells were released into inositol-free media, and cell-cycle progression over time was analyzed by FACS. In the absence of inositol, the *tgl3 tgl4* mutant entered the cell cycle 150 min after release into fresh media, in contrast to wild type (minus inositol), which showed a 2N peak (postreplication) at 120 min (Fig. S3). The delay in the lipase mutant in the absence of inositol indicates additive effects of inositol starvation and defective lipolysis on cell-cycle progression, both of which contribute to sphingolipid synthesis.

Lipolysis-Defective Mutants Accumulate Saturated and Unsaturated TG Species. Because the cell-cycle defect of *tgl3 tgl4* mutants was suppressed by supplementation with C14:0 and C16:0, we next investigated whether these specific FAs are indeed derived from TG breakdown during cell-cycle progression. Synchronized cells were harvested and total lipids were extracted and analyzed by ultra high performance liquid chromatography–electrospray ionization–mass spectrometry (UPLC–ESI–MS) over a period of 2 h (Fig. 2 and Fig. S4). In wild-type cells, TG species containing saturated FAs are present only in minor amounts (Fig. 2*A* and Fig. S4*A*). Throughout the cell cycle, TG molecular species containing saturated FAs steadily increased over time, whereas the major unsaturated species (containing three unsaturated FAs) declined, as expected, in the presence of the Tgl3 and Tgl4 lipases. This observation supports the notion that FA de novo synthesis contributes to the cellular lipid content during the cell cycle and that a minor fraction of the newly generated (saturated) FAs indeed feed into the TG pool. In wild-type cells, TG levels decreased by 30%; this decline was due to active lipolysis rather than simple dilution by cell division, which did not take place during the observed time window. The observed prevalent turnover of unsaturated TG species is consistent with the described in vitro specificity of the yeast TG lipases (12, 42). As expected and consistent with previous observations (4, 12, 42), *tgl3 tgl4* mutants had about threefold elevated TG levels (Fig. 2*B* and Fig. S4*B*); notably, despite the absence of the major lipases, TG levels significantly declined by ~10% during the first hour after entry into the cell cycle, indicating that additional TG lipases/acyltransferases may be active during this growth phase. Subsequently, TG levels increased again until the cell cycle was completed, which again reflects endogenous FA synthesis and deposition into TG, in the absence of lipolysis. Tgl3 and Tgl4 lipases appear to have a strong substrate preference for TG molecular species harboring three unsaturated FAs, which remain unaltered in the lipase mutants during the initial cell duplication (4, 12, 42). Most notably, however, fully saturated TG

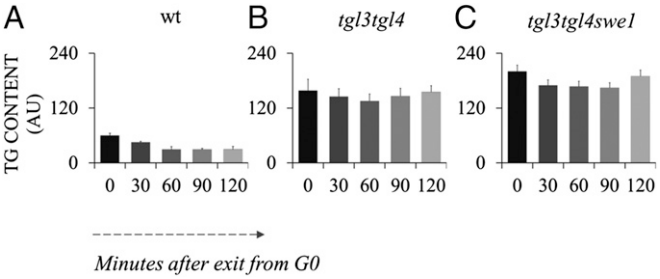

Fig. 2. TG content in wild-type, *tgl3 tgl4*, and *tgl3 tgl4 swe1* mutants during the cell cycle (see also Fig. S4). RediGrad synchronized G0 cells were released into fresh glucose containing minimal media, and 20 OD_{600} units were harvested at the indicated time points for lipid analysis. (*A*) Wild type. (*B*) *tgl3 tgl4* mutant. (*C*) *tgl3 tgl4 swe1* mutant. In wild type, total TG levels decreased over time. *tgl3 tgl4* and *tgl3 tgl4 swe1* mutants contain about threefold elevated TG levels compared with wild type; during the first 30 min into the cell cycle, some TG degradation was observed in the lipase mutants, indicating the presence of additional lipases/transacylases. Deletion of *SWE1* does not activate additional lipases. The slightly increased relative TG content in the *tgl3 tgl4 swe1* strain compared with *tgl3 tgl4* mutants may be due to the different cell sizes that affect OD_{600} readings to which TG content was normalized. Error bars indicate the SD of three independent experiments.

molecular species, including those harboring C14:0 and C16:0 acylresidues (TG 42:0, TG 48:0), were substantially increased in the *tgl3 tgl4* mutant (Fig. S4*B*). We conclude from this observation that a significant fraction of de novo synthesized saturated FAs is channeled into TG synthesis, before their modification by elongation/desaturation, and subsequently delivered into glycerophospholipids by a process that requires the activity of Tgl3 and Tgl4. This mechanism also explains why supplementation of these FAs bypasses the requirements for lipolysis for cell-cycle progression in the lipase mutants. Because maximum growth rates of *tgl3 tgl4* mutants are identical to wild-type cells (Fig. S1), TG accumulation per se does not impair growth, but rather TG-derived sphingolipid precursors become limiting upon cell-cycle entry from the stationary phase, in the absence of lipases and insufficient endogenous FA synthesis.

The Cell-Cycle Delay in the *tgl3 tgl4* Mutant Is Executed by the Checkpoint Kinase Swe1. As cells progress through the cell cycle, various checkpoints are activated during defined stages of cell division. Because lack of lipolysis delayed cell-cycle progression at the onset of bud formation, which is associated with actin polarization and morphology alterations, we hypothesized that the morphogenesis checkpoint kinase Swe1 (25, 30, 43) might play a role in executing this delay. In addition to its role in establishing actin polarity and functioning as a cell-cycle checkpoint (22, 29, 32), Swe1 was also identified in a large-scale study to be connected to sphingolipid metabolism by its genetic interaction with *LCB1*, encoding the catalytic subunit of SPT (44, 45). A related sphingolipid-associated checkpoint function of Swe1 was also reported in the context of inositol sphingolipase C (Isc1), which catalyzes the formation of bioactive ceramides from complex sphingolipids (46, 47). Based on these observations, Swe1 appeared as a likely candidate for regulating cell-cycle progression in response to altered lipolysis and the subsequent sphingolipid deficiencies. Indeed, additional deletion of *SWE1* in the *tgl3 tgl4* mutant background suppressed the G1/S phase delay, and the *tgl3 tgl4 swe1* triple mutant progressed through the cell cycle like wild type (Fig. 3*A*). These data therefore confirm that Swe1 kinase is the checkpoint that senses the lack of lipolysis and delays the cell cycle in the absence of saturated FA or long-chain sphingoid base supply. Previous studies have identified tyrosine 19 of the cyclin-dependent kinase Cdk1/Cdc28 as the specific phosphorylation site through which Swe1 regulates cell-cycle

progression (22). As expected, and similar to a Swe1 deletion, point mutation of Cdc28^{Y19F} also suppressed the cell-cycle delay in *TGL3 TGL4*-deficient cells (Fig. 3*A*). Bud emergence in the *tgl3 tgl4 swe1* and *tgl3 tgl4 cdc28^{Y19F}* mutants was restored to wild type as well (Fig. 3*B*). Because Swe1 is established as a regulator of entry into mitosis (22, 48), we next tested conditions under which Swe1 would also display a function in G1, as suggested by its negative regulatory role in *tgl3 tgl4* mutants. *SWE1* overexpression in vegetatively growing wild type induced a morphology defect—that is, mononucleate mother cells and nucleus-free elongated daughter cells—and a G2 arrest, consistent with published data (22, 30, 33, 49) (Fig. 3*C*). In contrast, *SWE1* overexpression in *tgl3 tgl4* mutants, however, induced a similar morphology defect but a G1 arrest; both phenotypes were not observed by additional mutation of the Swe1 phosphorylation site in Cdc28^{Y19}. From these experiments we conclude that Swe1 indeed becomes activated in G1 in the absence of lipolysis, supporting a previously unidentified function of this checkpoint kinase in cell-cycle regulation.

To further confirm the unexpected role of Swe1 in G1, we next characterized the appearance of cyclins and the phosphorylation status of Cdc28^{Y19} in strains lacking *tgl3 tgl4* lipases under various lipid supplementation conditions (Fig. 4 and Fig. S5). In the absence of lipolysis in *tgl3 tgl4* mutants, Cdk1/Cdc28 is phosphorylated already at 60 min after release of G0 cells into the cell cycle, before the onset of bud formation; this is in marked contrast to wild-type cells, which display Cdc28 phosphorylation only after 120 min, at the G2/M transition (Fig. 4*A*). Cdc28 phosphorylation in *tgl3 tgl4* mutant cells indeed responds to the presence of lipid precursors, palmitic acid, or long-chain base (PHS) in a cell-cycle–dependent manner. Consistent with our hypothesis, Cdc28 phosphorylation in the *tgl3 tgl4* mutant supplied with C16:0 or with PHS followed kinetics similar to wild-type cells (Fig. 4*A*). This further supports the notion that the cell-cycle delay in the absence of lipolysis is due to defective sphingolipid synthesis.

The cell-cycle delay of the *tgl3 tgl4* mutant is also reflected in the delayed appearance of the G1 cyclin Cln2 (50, 51), S-phase cyclin Clb5 (52, 53), and the G2 cyclin Clb2 (54, 55) (Fig. 4 *B*–*D*). Additional deletion of *SWE1*, mutation of the Swe1-dependent phosphorylation site of Cdc28^{Y19}, or supplementation of lipid precursors restored wild-type cell-cycle entry and progression. These data confirm a role of Swe1 in executing the delay in G0 exit in the absence of TG breakdown.

Swe1 Does Not Directly Regulate Lipolysis. Because deletion of *SWE1* in the lipase-deficient mutant suppressed the cell-cycle delay, we next investigated whether Swe1 directly affected lipid homeostasis and restored lipolysis by an unknown mechanism, in the absence of the major TG lipases Tgl3 and Tgl4. This, however, was not the case (Fig. 2*C* and Fig. S4*C*): Additional deletion of *SWE1* in the lipase-deficient strain did not significantly reduce but rather slightly increased TG content per OD_{600} unit, excluding the possibility that absence of the kinase bypasses the cellular requirement for Tgl3 and Tgl4 by activation of alternative TG lipases.

The Role of PP2A^{CDC55} Phosphatase in Regulating the Cell-Cycle Delay in *tgl3 tgl4* Mutant. Swe1 and Cdc28 kinases function in a positive feedback loop at G2/M (33) and are regulated by two phosphatases, PP2A^{Cdc55} and Mih1. Cdc55 was described to be active during early mitosis and regulates removal of the activating phosphorylation of Swe1, thus preventing the inactivation of Cdc28; these combined activities allow accumulation of a threshold level of active Cdc28. A *cdc55* mutation causes hyperphosphorylation of Swe1, indicating that PP2A^{Cdc55} is the primary phosphatase that acts on Swe1 during early mitosis (34). Of note, sphingolipids have previously been reported to be effectors of PP2A^{Cdc55} function (56, 57), supporting a role in regulating Swe1 activity. To further assess

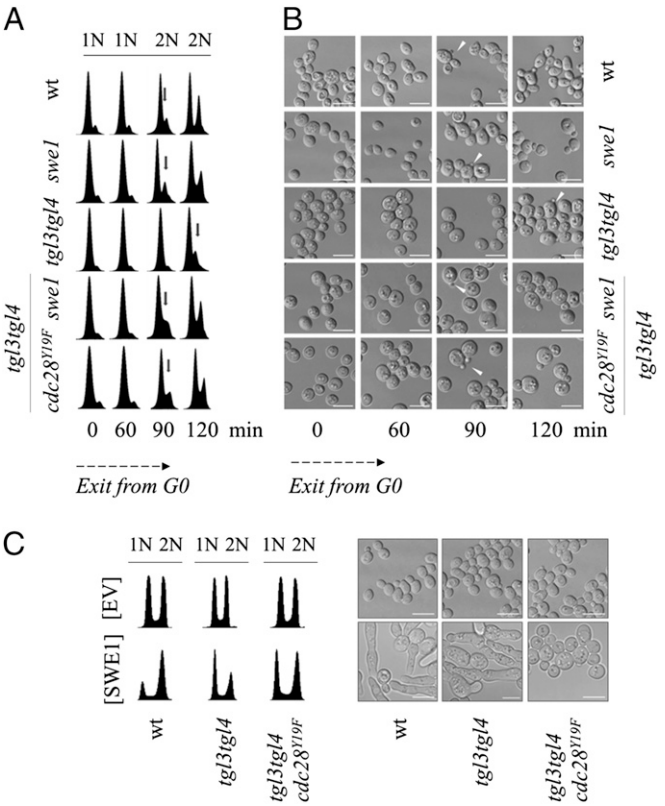

Fig. 3. The cell-cycle delay of the *tgl3 tgl4* mutant is mediated by the checkpoint kinase Swe1. RediGrad synchronized G0 cells were released into fresh glucose containing minimal media. (*A*) Cells were harvested at the indicated time points, and the DNA content was analyzed by FACS. The *tgl3 tgl4 swe1* and the *tgl3 tgl4 cdc28^{Y19F}* mutants enter the S phase 90 min after release into fresh medium, similar to wild type and the *swe1* mutant. (*B*) Bud formation in the mutants was analyzed by microscopy and indicated by white arrowheads. In wild-type, *swe1*, *tgl3 tgl4 swe1*, and *tgl3 tgl4 cdc28^{Y19F}* mutants, onset of bud formation occurs at 90 min after release into fresh glucose-containing media, in contrast to the *tgl3 tgl4* mutant, which shows a delay and appearance of buds and is seen only at 120 min after release. (*C*) Overexpression of *SWE1* extends the G1 cell-cycle delay in the lipase mutants. A logarithmic population of cells overexpressing *SWE1* was harvested and the DNA content analyzed by FACS. Wild type shows a larger population of premitotic (2N) cells compared with the *tgl3 tgl4* mutant, which shows a pronounced 1N peak (prereplication) upon *SWE1* overexpression. The *tgl3 tgl4 cdc28^{Y19F}* mutant lacking the Swe1-specific phosphorylation site in Cdc28 shows an equal distribution of cells in the G1 and G2 phases similar to the empty vector (EV) controls, characteristic for an unsynchronized population of dividing cells. The morphology defect induced by *SWE1* overexpression in wild-type and lipase mutant is absent in the *tgl3 tgl4 cdc28^{Y19F}* mutant (*C*, *Right*). (Scale bar, 10 μm.)

the role of Swe1 in regulating cell-cycle progression at the G1/S boundary, we next investigated the impact of the phosphatase PP2A^{Cdc55}. Deletion of *CDC55* delayed entry into the cell cycle by 30 min compared with wild type, indicating a role of Cdc55 also in G1/S (Fig. 5 and Fig. S6). Deletion of *CDC55* in the *tgl3 tgl4* background extended this delay further by ~60 min, indicating additive effects. This is not surprising because Cdc55 has been reported to influence the stability of the G1 cyclin Cln2, thereby exhibiting a major impact on the timing of the G1/S transition (58). The *swe1 cdc55* double mutant, on the other hand, behaved like wild type, confirming that Swe1 phosphorylation/activity is responsible for controlling the cell-cycle progression at G1/S. Furthermore, supplementation of PHS did not affect cell-cycle progression of mutants deleted for *CDC55* (Fig. 5 and Fig. S6), providing further evidence that activation of Cdc55 and subsequent

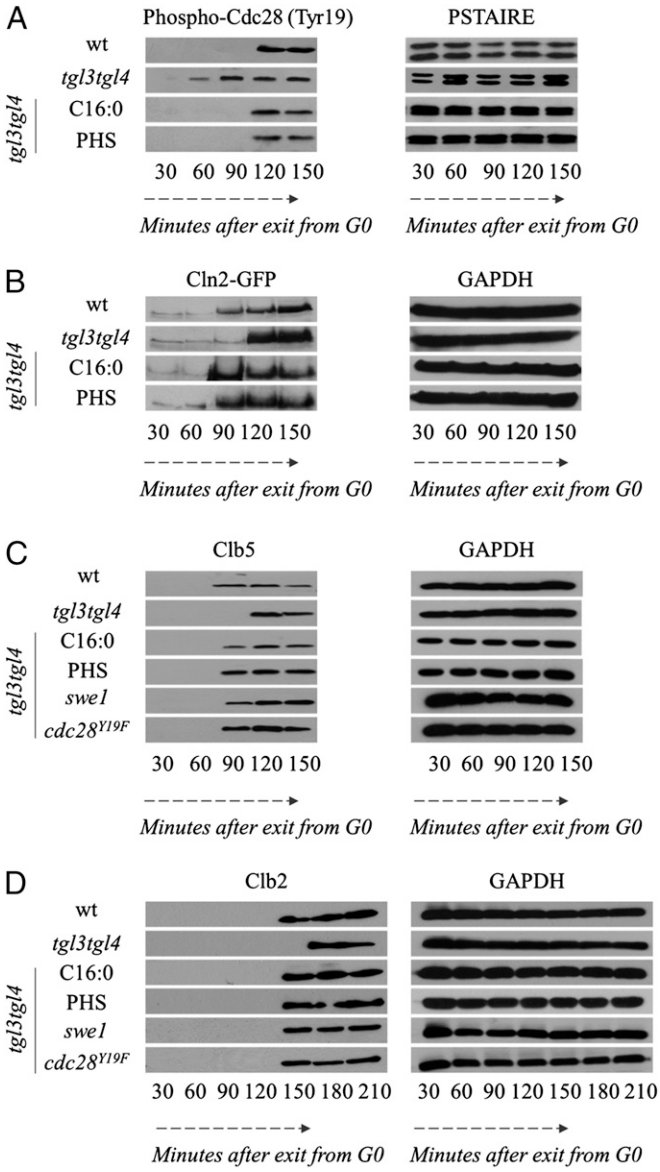

Fig. 4. The cell-cycle delay mediated by Swe1-dependent phosphorylation of Cdc28 in the *tgl3 tgl4* mutant occurs at G1. At the indicated time points, whole-cell extracts were prepared for Western blot analysis, using antibodies against phospho-cdc2 (Tyr15) to probe Cdc28^{Y19} phosphorylation, α-PSTAIRE to detect total levels of Cdc28, and α-GFP to detect Cln2-GFP, α-Clb5, and α-Clb2. (*A*) The cell-cycle delay in the *tgl3 tgl4* mutant results from the inhibitory phosphorylation of Cdc28: In wild type, Cdc28^{Y19} phosphorylation is detectable at G2/M, 120 min after release into fresh media. In contrast, in the *tgl3 tgl4* mutant, phospho-Cdc28^{Y19} is detectable already 60 min after release into fresh medium. Upon supplementation of PHS (1 μM in 0.2% tergitol) or C16:0 (0.025% in 1% tergitol) to the *tgl3 tgl4* mutant, phospho-Cdc28^{Y19} is detectable only 120 min after release, similar to wild type. (*B*) Low levels of Cln2-GFP are detectable in G0 cells and peak at the G1/S transition, after 90 min in wild type. In the *tgl3 tgl4* mutant, Cln2 levels peak after 120 min; wild-type appearance of Cln2 is restored in these mutants in the presence of C16:0 or PHS. (*C*) The appearance of Clb5 coincides with the initiation of DNA replication. S phase in the *tgl3 tgl4* mutant is initiated 120 min after release; this is in contrast to wild-type, *tgl3 tgl4* mutants supplemented with C16:0 or PHS, *tgl3 tgl4 swe1* or *tgl3 tgl4 cdc28^{Y19F}* mutants, in which it is initiated already 90 min after release. (*D*) Clb2 marks the entry into mitosis. Clb2 is first detectable in synchronized wild type at 150 min, compared with the *tgl3 tgl4* mutant in which it is first detected 180 min after release. The *tgl3 tgl4* mutant supplemented with C16:0 or PHS, *tgl3 tgl4 swe1*, and *tgl3 tgl4 cdc28^{Y19F}* mutants behave like wild type. GAPDH was used as a loading control for *B*–*D*. Representative blots from three independent experiments are shown.

inactivation of Swe1 are dependent on sphingolipids. This is also consistent with a previous study that showed that the PP2A^{Cdc55}–Swe1 cascade is a downstream target of the sphingolipid, phytoceramide (59). We conclude that deletion of the regulatory subunit of PP2A^{Cdc55} makes the cells unresponsive to the availability of sphingolipids (SLs), which results in pertained activation of Swe1 and extension of the G1/S phase. In contrast, the Mih1 phosphatase that is required to remove the inhibitory phosphorylation of Cdc28 in the G2/M phase of the cell cycle (27, 28, 43) neither positively nor negatively affected the cell-cycle progression of the lipase-deficient mutant at the G1/S boundary (Fig. 5 and Fig. S6). Of note, Mih1 activity was previously implicated in regulating cell-cycle progression in response to altered secretion, which is also required for delivery of membrane lipids to the expanding plasma membrane in the growing bud. A block in secretion in a *sec6-4* temperature-sensitive mutant also triggers a Swe1-dependent checkpoint but during early mitosis (60). Thus, Swe1 may indeed function as a lipid-dependent checkpoint at multiple stages of the cell cycle; here, we show that it operates as a lipolysis-regulated checkpoint kinase at the G1/S transition of the cell cycle and that its activity is regulated by the PP2A^{Cdc55} phosphatase in a lipid-dependent manner.

G0 to G1/S Lipid-Dependent Regulation of Cell-Cycle Progression: A Model. Both plasma membrane and also intracellular membrane proliferation in growing cells demand net phospholipid synthesis, which is satisfied not only by de novo production of FAs but also by recycling of storage lipids—that is, TG. In addition, delivery of cell wall components through the secretory pathway relies on vesicular trafficking, linking cell-cycle progression to the regulation of key steps of lipid metabolism and membrane growth (6, 8, 38, 61, 62). In our experimental setup, we investigated the requirement of lipolysis to regulate recovery from quiescence and exit from G0 into a new cell cycle. Quiescence is important for survival under starvation conditions, and a hallmark of quiescent cells is their ability to synchronously enter the mitotic cycle (6, 63). G0 cells significantly differ in their physiology from vegetatively growing cells with respect to metabolism, protein synthesis, and membrane trafficking (64–67).

Mutants lacking the two major TG lipases Tgl3 and Tgl4 show a delayed entry of cells from G0 into the cell cycle (6) (Fig. 1), which can be rescued by supplementation with C14:0 or C16:0 FAs or PHS, which are all precursors for the synthesis of sphingolipids (Fig. 1). The specific lipid requirements upon entry into the growth cycle appear to be different from vegetatively growing cells, as none of the mutants display a significant growth defect during logarithmic growth (Fig. S1 *A* and *B*). This is not unprecedented, as mutants lacking Gcs1, a regulator of the phospholipase D, Spo14 (68), or the FA activator Faa1 (69), are defective in exiting quiescence; neither *spo14* nor *faa1* mutants, however, display a significant vegetative growth phenotype, consistent with the notion that G0 reflects a metabolic state rather than a cell-cycle state (70, 71).

The cell-cycle delay of the *tgl3 tgl4* mutants was efficiently suppressed by the additional deletion of *SWE1*; this kinase was previously described as a checkpoint that monitors actin polarization, which precedes bud formation (32, 70, 72). Because in our setup both DNA replication and bud formation are concomitantly delayed, the checkpoint role of Swe1 kinase is not unexpected. The delayed accumulation of late G1 cyclins (Clb5 and Cln2) and the G2 cyclin (Clb2) further demonstrates that absence of lipolysis results in a delayed onset of the G1/S transition (Fig. 4). This delay is clearly regulated by the activity of Swe1 that inhibits Cdc28; the nature of the Cdc28/cyclin complex that is inhibited or absent at the G0 exit in the absence of lipolysis remains to be determined (Fig. 4). We thus propose the following model for lipolysis-regulated cell-cycle progression (Fig. 6): When cells are released from the G0 phase into fresh glucose-containing media, Cdc28 phosphorylates and activates

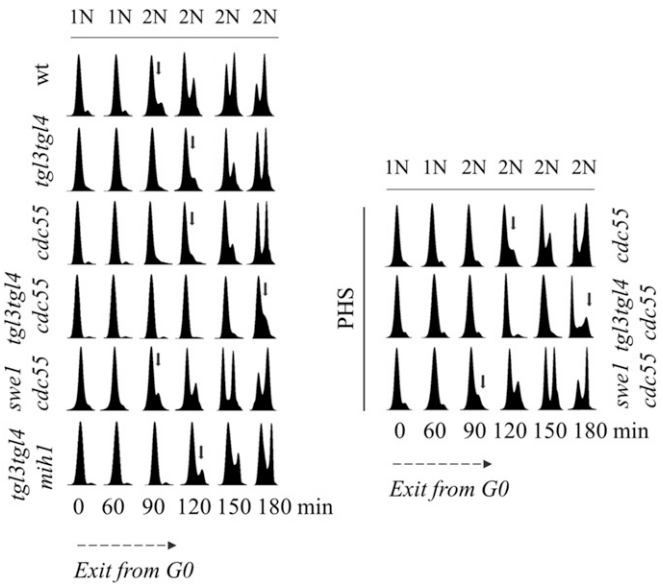

Fig. 5. Modulation of Swe1 kinase activity affects lipolysis-dependent G1/S transition. Deletion of the Swe1 phosphatase $PP2A^{Cdc55}$ affects cell-cycle progression in the lipase mutants. RediGrad synchronized G0 cells were released into fresh glucose-containing media. As indicated by arrows, the *cdc55* mutant strain enters the cell cycle ~120 min after release into fresh media. Deletion of *CDC55* in the *tgl3 tgl4* mutant further extended the initiation of the S phase, whereas the *swe1 cdc55* mutant behaved like wild type. The supplementation of PHS (1 μM in 0.2% tergitol) to the mutants lacking $PP2A^{CDC55}$ did not affect cell-cycle progression. Deletion of *MIH1* in the *tgl3 tgl4* mutant has no influence on the cell-cycle progression. The experiments were independently repeated three times.

Tgl4 lipase; in conjunction with Tgl3, lipolytic TG breakdown provides FAs for the synthesis of sphingolipids that activate $PP2A^{Cdc55}$, which in turn inactivates Swe1 and leaves the control point unchecked. As a result, Cdc28 is active and G1/S transition proceeds normally (Fig. 6). When *tgl3 tgl4* mutant cells are released from G0 into fresh media, Cdc28 cannot induce lipolysis and limited de novo FA synthesis is the sole provider of sphingolipid precursors (Fig. 6). Under this condition, Cdc28 phosphorylates and activates Swe1 kinase, which in turn phosphorylates and inhibits Cdc28, thereby triggering the checkpoint and inducing a G1/S phase delay. In the absence of lipolysis-derived sphingolipids, impaired $PP2A^{Cdc55}$ function fails to remove the activating phosphorylation of Swe1 until adequate levels of lipid metabolites become available.

Materials and Methods

Strains and Growth Conditions. The *Saccharomyces cerevisiae* strains used in this study are listed in Table 1. Double mutants were constructed by standard genetic crosses and by targeted gene deletion by homologous recombination. *cdc55* deletion mutants were generated by replacing the ORF with a Nat^R cassette. Gene deletions (Euroscarf) were verified by colony PCR with the appropriate up-tag and down-tag primers. Strain RSY342 (*MATa bar1 cdc28^{Y19F}::TRP1 GAL1-SWE1^{myc}::URA3*) was a kind gift from Daniel Lew's laboratory, Department of Pharmacology and Cancer Biology, Duke University Medical Center. Because the strain had a genetic background different from the BY strains, the genomic DNA was used as a template and *cdc28^{Y19F}* was amplified using primers 5′-GACTAATGCATCATGGCTTATGTATTATACTTGCTTATGT-3′ and 5′-ACTAATGCATGCTCCTAACGGTTGGTCCTTTGGAATACC-3′. The fragment with flanking Nsi1 restriction enzyme sites was ligated into the pSH47/NAT^R plasmid and was amplified using the primers 5′-TTTTTATACAATACATATATATATATATATATATATATTTACAAGAAAAGACATGGAGGCCCAGAATACCC-3′ and 5′-GCTCCTAACGGTTGGTCCTTTGGAATACC-3′ such that the Nat^R cassette was inserted downstream of the mutated *CDC28* gene. This construct was chromosomally integrated into wild-type and *tgl3 tgl4* mutants, and the transformed strains were selected for ClonNAT resistance; the mutation was confirmed by sequencing.

For constructing an *N*-terminal fusion with GST on an episomal plasmid, the *SWE1* gene was amplified as a BamHI-NotI fragment by PCR, using genomic DNA as the template and primers 5′-GACTAGGATCCAGTTCTTTGGACGAGGATGAAGAG-3′ and 5′-GACTAGCGGCCGCTCATATAAAAAATTTTGGCTTAGGTCCAAA-3′. The PCR fragment was inserted into the respective restriction sites of plasmid pYEX4T-1 (Clontech) downstream of the copper-inducible promoter.

A chromosomally integrated *CLN2*-monomeric GFP (mGFP) fusion was constructed by amplifying the mGFP-NatMX6 fragment from a modified pFA6a-GFP (S65T)–KanMX6 plasmid (73) in which the KanMX6 cassette had been replaced by a ClonNAT resistance cassette and the GFP had been changed to mGFP. The following primers were used: 5′-GCAGTGCCTCATCTTTAATTTCTTTTGGTATGGGCAATACCCAAGTAATAGTGAGCAAGGGCGAGGAGCTG-3′ and 5′-TTTTGGTACGTTTGGCAAATTGGCATTCATTTATCATGAAAAGAACAGGATTAGGGGCAGGGCATGCTCATG-3′. The strains harboring the chromosomally integrated *CLN2*-mGFP fragment were obtained by linear transformation and selection for ClonNAT resistance. Correct integration of the GFP was verified by colony PCR.

Yeast cells were grown in YPD [extract, peptone, dextrose (glucose)] medium containing 1% yeast extract, 2% (wt/vol) peptone, and 2% (wt/vol) glucose, or in yeast nitrogen base (YNB) minimal medium (MM) containing 0.67% yeast nitrogen base, 2% (wt/vol) glucose, and the respective amino acids and nucleo bases; for experiments lacking inositol, threonine was omitted from the amino acid stock. Solid media had the same composition plus 2% (wt/vol) agar (74). Yeast strains carrying expression plasmids were maintained in uracil drop-out medium. YPD plates containing 200 mg/L G418 (Geneticin; Calbiochem) or 100 mg/L ClonNAT (nourseothricin; Sigma) were used to select for KanMX or Nat^R markers, respectively. Sporulation

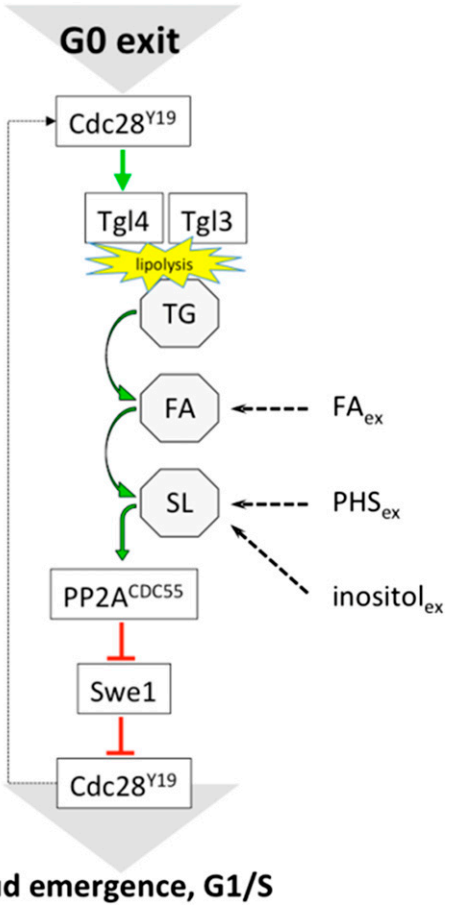

Fig. 6. Lipid-dependent regulation of cell-cycle progression by the Swe1 kinase. Limited availability of lipid precursors (in particular SLs) in quiescent cells activates the checkpoint kinase Swe1 and induces a cell-cycle delay at the G1/S transition by phosphorylating $Cdk1/Cdc28^{Y19}$. Ex, exogenous supply; FA, fatty acid; PHS, phytosphingosine; SL, sphingolipids. See *G0 to G1/S Lipid-Dependent Regulation of Cell-Cycle Progression: A Model* for details.

Table 1. Strains used in this study

Strain	Genotype	Source
RSY342	*Mata bar1 cdc28^{Y19F}::TRP1 GAL1-SWE1^{myc}::URA3*	Ref. 31
BY4742	*MATα his3Δ1 leu2Δ0 lys2Δ0 ura3Δ0*	Euroscarf
YCK1158	*MATa his3Δ1 leu2Δ0 lys2Δ0 ura3Δ0 tgl3::KanMX4 tgl4::KanMX4*	Ref. 6
YNC001	*MATα his3Δ1 leu2Δ0 lys2Δ0 ura3Δ0 swe1::KanMX4*	Open Biosystems
YNC002	*MATa his3Δ1 leu2Δ0 lys2Δ0 ura3Δ0 tgl3::KanMX4 tgl4::KanMX4 swe1::Nat^R*	This study
YNC003	*MATα his3Δ1 leu2Δ0 lys2Δ0 ura3Δ0 cdc28^{Y19F}-Nat^R*	This study
YNC004	*MATα his3Δ1 leu2Δ0 lys2Δ0 ura3Δ0 tgl3::KanMX4 tgl4::KanMX4 cdc28^{Y19F}::Nat^R*	This study
YNC005	*MATα his3Δ1 leu2Δ0 lys2Δ0 ura3Δ0 cdc55::Nat^R*	This study
YNC006	*MATa his3Δ1 leu2Δ0 lys2Δ0 ura3Δ0 tgl3::KanMX4 tgl4::KanMX4 cdc55::Nat^R*	This study
YNC007	*MATα his3Δ1 leu2Δ0 lys2Δ0 ura3Δ0 swe1::KanMX4 cdc55::Nat^R*	This study
YNC008	*MATα his3Δ1 leu2Δ0 lys2Δ0 ura3Δ0* (transformed with pYEX4T-1-SWE1)	This study
YNC009	*MATa his3Δ1 leu2Δ0 lys2Δ0 ura3Δ0 tgl3::KanMX4 tgl4::KanMX4* (transformed with pYEX4T-1-SWE1)	This study
YNC010	*MATα his3Δ1 leu2Δ0 lys2Δ0 ura3Δ0 tgl3::KanMX4 tgl4::KanMX4 cdc28^{Y19F}::Nat^R* (transformed with pYEX4T-1-SWE1)	This study
YNC011	*MATa his3Δ1 leu2Δ0 lys2Δ0 ura3Δ0 tgl3::KanMX4 tgl4::KanMX4 mih1::KanMX4*	This study
YNC012	*MATα his3Δ1 leu2Δ0 lys2Δ0 ura3Δ0 Cln2-GFP::Nat^R*	This study
YNC013	*MATa his3Δ1 leu2Δ0 lys2Δ0 ura3Δ0 tgl3::KanMX4 tgl4::KanMX4 Cln2-GFP::Nat^R*	This study

medium contained 0.25% yeast extract, 0.1% glucose, and 1% potassium acetate. Stocks of myristic acid (Fluka) and palmitic acid (Sigma) were prepared in 10% (vol/vol) tergitol (Sigma) and supplemented to YNB MM at a final concentration of 0.025%. PHS (Avanti Lipids) stock was prepared in methanol and supplemented into YNB containing 0.2% tergitol at a final concentration of 1 μM. Expression of GST-*SWE1* under the control of the *CUP1* promoter was induced by the addition of 0.5 mM copper sulfate to the medium. Yeast strains were cultivated at 30 °C in a shaker incubator.

Synchronization of Cells by RediGrad Centrifugation. Cells were cultivated to the stationary phase for 7 d in YPD medium [1% yeast extract, 2% (wt/vol) peptone, 2% (wt/vol) dextrose], and quiescent G0 cells were harvested by RediGrad centrifugation as described (6, 63). In brief, a density gradient was established by using nine parts of RediGrad ("Percoll Plus," GE Healthcare Life Sciences) and one part of 1.5 M NaCl followed by centrifugation at 40,000 × *g* for 15 min. Cells were resuspended in 1 mL of 50 mM Tris·HCl (pH 7.5) and carefully layered onto the formed gradient and centrifuged again at 450 × *g* for 1 h. The quiescent/G0 cells were collected from the bottom of the gradient and washed well with 50 mM Tris·HCl (pH 7.5) before use.

Fluorescence-Activated Cell Sorting Analysis. Cell-cycle progression was analyzed by FACS as described (6). At the indicated time points, cell culture aliquots were harvested, fixed in 70% ethanol, and stored at 4 °C; fixed cells were treated with 10 mg/mL RNaseA (Roche) in 50 mM Tris·HCl (pH 8.0) for 4 h at 37 °C, followed by Proteinase K (2 mg/mL) treatment at 50 °C for 60 min. Cells were pelleted and resuspended in PBS (pH 8.0). The DNA was stained with 1 mM SYTOX Green (Invitrogen, Inc.) for 10 min; cells were briefly sonicated at low intensity in a sonicator bath and analyzed using a FACSaria flow cytometry system (BD Biosciences). The DNA profiles were analyzed using settings appropriate for the detection of Sytox Green stain.

Preparation of Yeast Whole-Cell Extracts and Immunoblotting. Total cell extracts were prepared as described by Baerends et al. (75). In brief, synchronized cells were released into fresh media; 3 OD_{600} units of cells were harvested at the indicated time points and incubated with 400 μL of 12.5% (wt/vol) trichloroacetic acid (TCA) at –80 °C for at least 30 min to allow protein precipitation. TCA was removed by centrifugation, and the cell pellets were washed twice with 80% (vol/vol) ice-cold acetone, air-dried, and dissolved in 1% SDS/0.1N NaOH. We added 1× SDS loading buffer, and samples were boiled for 5 min before loading onto polyacrylamide gels. Proteins were resolved on 10% (wt/vol) SDS polyacrylamide gels and blotted onto nitrocellulose membranes (Bio-Rad). Anti-rabbit phospho-cdc2 (Tyr15) antibody (Cell Signaling Technology) was used to detect phosphorylated Cdc28^{Y19}, and anti-human PSTAIRE antibody, which detects total Cdk1/Cdc28 (Santa Cruz Biotechnology), was used as a loading control. Anti-rabbit α-Clb5 (76) and anti-rabbit α-Clb2 antibodies were a kind gift from Adam Rudner, Ottawa Institute of Systems Biology, University of Ottawa, and were used as previously described (77). For Western blots of Cln2-mGFP, 10 OD_{600} units of cells were harvested at the indicated time points and processed as described above. Mouse anti-GFP antibody (Roche) was used for detection of Cln2-mGFP. Horseradish peroxidase-conjugated anti-rabbit IgG (Santa Cruz Biotechnology) and anti-mouse IgG (Pierce, Thermo Fisher Scientific) were the secondary antibodies, and ECL Western Blotting Substrate (Pierce) was used for detection.

Lipid Analysis. Cells obtained by RediGrad centrifugation were inoculated into fresh synthetic complete YNB media and harvested at indicated time points, snap frozen in liquid nitrogen, and stored at –80 °C until lipid extraction was performed. An internal standard mix was added (78), and lipids were extracted according to Folch et al. after glass bead homogenization of cells (79). The lipid extracts were analyzed by UPLC–ESI–quadrupol time-of-flight (qTOF)–MS (78), and chromatograms and mass spectra were evaluated using Waters MassLynx and Lipid Data Analyzer Software (80).

Microscopy. RediGrad synchronized or logarithmically growing cells were harvested and resuspended in 100 μL of 4% paraformaldehyde/sucrose solution and incubated at room temperature for 15 min. The cells were then washed with 500 μL of K-PO_4/sorbitol buffer (pH 7.5), resuspended in 100 μL of the same solution, and stored at 4 °C until further use. Before use, samples were briefly sonicated and imaging was performed using a Leica SP2 confocal microscope (Leica Microsystems, Inc.) using a 100× NA 1.4 oil objective and differential interference contrast optics.

Growth Curves and Analysis of Growth Phenotypes by Serial Dilution Drop Tests. Yeast strains were precultured in YPD media for 48 h, rediluted to 0.1 OD_{600} units/mL in 50 mL MM, and grown at 30 °C. Growth was monitored by measuring OD_{600} every 1.5 h for 15 h. For plate tests, yeast strains were cultured overnight at 30 °C in MM, and 10 OD_{600} units of cells were harvested and serially diluted in water. Then, 5 μL of these serial dilutions were dropped onto MM agar plates; supplemented with 1 μM PHS (0.2% tergitol), 0.25% C16:0 (1% tergitol), and 200 ng/mL myriocin (in DMSO); and incubated at 30 °C, 20 °C, or 39 °C, as indicated.

ACKNOWLEDGMENTS. We thank Dr. Daniel J. Lew (Department of Pharmacology and Cancer Biology, Duke University Medical Center) and Dr. Brenda Andrews (Terrence Donnelly Centre for Cellular & Biomolecular Research, University of Toronto) for strains and plasmids, Dr. Adam Rudner (Ottawa Institute of Systems Biology, University of Ottawa) for antibodies and experimental advice, Dr. Tobias Eisenberg (Institute of Molecular Biosciences, University of Graz) for help with FACS, and Dr. Christoph F. Kurat (Cancer Research UK) and members of the Kohlwein laboratory for critical reading of the manuscript and helpful suggestions. Financial support by grants of the Fonds zur Förderung der wissenschaftlichen Forschung (FWF) (Project F3005 LIPOTOX and PhD program Molecular Enzymology W901) and NAWI Graz (to S.D.K.); a stipend by the Basque Government (to A.C.-S.); and a stipend by the Vice-Rectorate for Human Resources Management and Gender Equality of the University of Graz (to N.C.) is gratefully acknowledged.

1. Jackowski S (1996) Cell cycle regulation of membrane phospholipid metabolism. *J Biol Chem* 271(34):20219–20222.
2. Santos-Rosa H, Leung J, Grimsey N, Peak-Chew S, Siniossoglou S (2005) The yeast lipin Smp2 couples phospholipid biosynthesis to nuclear membrane growth. *EMBO J* 24(11):1931–1941.
3. Choi HS, et al. (2012) Pho85p-Pho80p phosphorylation of yeast Pah1p phosphatidate phosphatase regulates its activity, location, abundance, and function in lipid metabolism. *J Biol Chem* 287(14):11290–11301.
4. Kurat CF, et al. (2006) Obese yeast: Triglyceride lipolysis is functionally conserved from mammals to yeast. *J Biol Chem* 281(1):491–500.
5. Zimmermann R, et al. (2004) Fat mobilization in adipose tissue is promoted by adipose triglyceride lipase. *Science* 306(5700):1383–1386.
6. Kurat CF, et al. (2009) Cdk1/Cdc28-dependent activation of the major triacylglycerol lipase Tgl4 in yeast links lipolysis to cell-cycle progression. *Mol Cell* 33(1):53–63.
7. Henry SA, Kohlwein SD, Carman GM (2012) Metabolism and regulation of glycerolipids in the yeast Saccharomyces cerevisiae. *Genetics* 190(2):317–349.
8. Pascual F, Carman GM (2013) Phosphatidate phosphatase, a key regulator of lipid homeostasis. *Biochim Biophys Acta* 1831(3):514–522.
9. Csaki LS, et al. (2013) Lipins, lipinopathies, and the modulation of cellular lipid storage and signaling. *Prog Lipid Res* 52(3):305–316.
10. Oelkers P, Cromley D, Padamsee M, Billheimer JT, Sturley SL (2002) The DGA1 gene determines a second triglyceride synthetic pathway in yeast. *J Biol Chem* 277(11):8877–8881.
11. Sorger D, Daum G (2002) Synthesis of triacylglycerols by the acyl-coenzyme A:diacylglycerol acyltransferase Dga1p in lipid particles of the yeast Saccharomyces cerevisiae. *J Bacteriol* 184(2):519–524.
12. Athenstaedt K, Daum G (2005) Tgl4p and Tgl5p, two triacylglycerol lipases of the yeast Saccharomyces cerevisiae are localized to lipid particles. *J Biol Chem* 280(45):37301–37309.
13. Kienesberger PC, Oberer M, Lass A, Zechner R (2009) Mammalian patatin domain containing proteins: A family with diverse lipolytic activities involved in multiple biological functions. *J Lipid Res* 50(Suppl):S63–S68.
14. Kohlwein SD (2010) Triacylglycerol homeostasis: Insights from yeast. *J Biol Chem* 285(21):15663–15667.
15. Kohlwein SD, Veenhuis M, van der Klei IJ (2013) Lipid droplets and peroxisomes: Key players in cellular lipid homeostasis or a matter of fat—Store 'em up or burn 'em down. *Genetics* 193(1):1–50.
16. Rajakumari S, Daum G (2010) Multiple functions as lipase, steryl ester hydrolase, phospholipase, and acyltransferase of Tgl4p from the yeast Saccharomyces cerevisiae. *J Biol Chem* 285(21):15769–15776.
17. Rajakumari S, Daum G (2010) Janus-faced enzymes yeast Tgl3p and Tgl5p catalyze lipase and acyltransferase reactions. *Mol Biol Cell* 21(4):501–510.
18. Gaspar ML, Hofbauer HF, Kohlwein SD, Henry SA (2011) Coordination of storage lipid synthesis and membrane biogenesis: Evidence for cross-talk between triacylglycerol metabolism and phosphatidylinositol synthesis. *J Biol Chem* 286(3):1696–1708.
19. Zanghellini J, et al. (2008) Quantitative modeling of triacylglycerol homeostasis in yeast—Metabolic requirement for lipolysis to promote membrane lipid synthesis and cellular growth. *FEBS J* 275(22):5552–5563.
20. Yasutis KM, Kozminski KG (2013) Cell cycle checkpoint regulators reach a zillion. *Cell Cycle* 12(10):1501–1509.
21. Haase SB, Wittenberg C (2014) Topology and control of the cell-cycle-regulated transcriptional circuitry. *Genetics* 196(1):65–90.
22. Lew DJ (2003) The morphogenesis checkpoint: How yeast cells watch their figures. *Curr Opin Cell Biol* 15(6):648–653.
23. Nurse P, Thuriaux P, Nasmyth K (1976) Genetic control of the cell division cycle in the fission yeast Schizosaccharomyces pombe. *Mol Gen Genet* 146(2):167–178.
24. Nurse P (1975) Genetic control of cell size at cell division in yeast. *Nature* 256(5518):547–551.
25. Gould KL, Nurse P (1989) Tyrosine phosphorylation of the fission yeast cdc2+ protein kinase regulates entry into mitosis. *Nature* 342(6245):39–45.
26. Russell P, Nurse P (1986) cdc25+ functions as an inducer in the mitotic control of fission yeast. *Cell* 45(1):145–153.
27. Gautier J, Solomon MJ, Booher RN, Bazan JF, Kirschner MW (1991) cdc25 is a specific tyrosine phosphatase that directly activates p34cdc2. *Cell* 67(1):197–211.
28. Dunphy WG, Kumagai A (1991) The cdc25 protein contains an intrinsic phosphatase activity. *Cell* 67(1):189–196.
29. Sia RA, Herald HA, Lew DJ (1996) Cdc28 tyrosine phosphorylation and the morphogenesis checkpoint in budding yeast. *Mol Biol Cell* 7(11):1657–1666.
30. Booher RN, Deshaies RJ, Kirschner MW (1993) Properties of Saccharomyces cerevisiae wee1 and its differential regulation of p34CDC28 in response to G1 and G2 cyclins. *EMBO J* 12(9):3417–3426.
31. Sia RA, Bardes ES, Lew DJ (1998) Control of Swe1p degradation by the morphogenesis checkpoint. *EMBO J* 17(22):6678–6688.
32. McMillan JN, Sia RA, Lew DJ (1998) A morphogenesis checkpoint monitors the actin cytoskeleton in yeast. *J Cell Biol* 142(6):1487–1499.
33. Harvey SL, Charlet A, Haas W, Gygi SP, Kellogg DR (2005) Cdk1-dependent regulation of the mitotic inhibitor Wee1. *Cell* 122(3):407–420.
34. Harvey SL, et al. (2011) A phosphatase threshold sets the level of Cdk1 activity in early mitosis in budding yeast. *Mol Biol Cell* 22(19):3595–3608.
35. Yang H, Jiang W, Gentry M, Hallberg RL (2000) Loss of a protein phosphatase 2A regulatory subunit (Cdc55p) elicits improper regulation of Swe1p degradation. *Mol Cell Biol* 20(21):8143–8156.
36. Asano S, et al. (2005) Concerted mechanism of Swe1/Wee1 regulation by multiple kinases in budding yeast. *EMBO J* 24(12):2194–2204.
37. McMillan JN, Theesfeld CL, Harrison JC, Bardes ES, Lew DJ (2002) Determinants of Swe1p degradation in Saccharomyces cerevisiae. *Mol Biol Cell* 13(10):3560–3575.
38. McCusker D, et al. (2007) Cdk1 coordinates cell-surface growth with the cell cycle. *Nat Cell Biol* 9(5):506–515.
39. Rajakumari S, Rajasekharan R, Daum G (2010) Triacylglycerol lipolysis is linked to sphingolipid and phospholipid metabolism of the yeast Saccharomyces cerevisiae. *Biochim Biophys Acta* 1801(12):1314–1322.
40. Miyake Y, Kozutsumi Y, Nakamura S, Fujita T, Kawasaki T (1995) Serine palmitoyltransferase is the primary target of a sphingosine-like immunosuppressant, ISP-1/myriocin. *Biochem Biophys Res Commun* 211(2):396–403.
41. Hanscho M, et al. (2012) Nutritional requirements of the BY series of Saccharomyces cerevisiae strains for optimum growth. *FEMS Yeast Res* 12(7):796–808.
42. Athenstaedt K, Daum G (2003) YMR313c/TGL3 encodes a novel triacylglycerol lipase located in lipid particles of Saccharomyces cerevisiae. *J Biol Chem* 278(26):23317–23323.
43. Russell P, Moreno S, Reed SI (1989) Conservation of mitotic controls in fission and budding yeasts. *Cell* 57(2):295–303.
44. Costanzo M, et al. (2010) The genetic landscape of a cell. *Science* 327(5964):425–431.
45. Sharifpoor S, et al. (2012) Functional wiring of the yeast kinome revealed by global analysis of genetic network motifs. *Genome Res* 22(4):791–801.
46. Matmati N, Kitagaki H, Montefusco D, Mohanty BK, Hannun YA (2009) Hydroxyurea sensitivity reveals a role for ISC1 in the regulation of G2/M. *J Biol Chem* 284(13):8241–8246.
47. Tripathi K, Matmati N, Zheng WJ, Hannun YA, Mohanty BK (2011) Cellular morphogenesis under stress is influenced by the sphingolipid pathway gene ISC1 and DNA integrity checkpoint genes in Saccharomyces cerevisiae. *Genetics* 189(2):533–547.
48. Lew DJ (2000) Cell-cycle checkpoints that ensure coordination between nuclear and cytoplasmic events in Saccharomyces cerevisiae. *Curr Opin Genet Dev* 10(1):47–53.
49. Kellogg DR (2003) Wee1-dependent mechanisms required for coordination of cell growth and cell division. *J Cell Sci* 116(Pt 24):4883–4890.
50. Hadwiger JA, Wittenberg C, Richardson HE, de Barros Lopes M, Reed SI (1989) A family of cyclin homologs that control the G1 phase in yeast. *Proc Natl Acad Sci USA* 86(16):6255–6259.
51. Wittenberg C, Sugimoto K, Reed SI (1990) G1-specific cyclins of S. cerevisiae: Cell cycle periodicity, regulation by mating pheromone, and association with the p34CDC28 protein kinase. *Cell* 62(2):225–237.
52. Epstein CB, Cross FR (1992) CLB5: A novel B cyclin from budding yeast with a role in S phase. *Genes Dev* 6(9):1695–1706.
53. Schwob E, Nasmyth K (1993) CLB5 and CLB6, a new pair of B cyclins involved in DNA replication in Saccharomyces cerevisiae. *Genes Dev* 7(7A):1160–1175.
54. Fitch I, et al. (1992) Characterization of four B-type cyclin genes of the budding yeast Saccharomyces cerevisiae. *Mol Biol Cell* 3(7):805–818.
55. Surana U, et al. (1991) The role of CDC28 and cyclins during mitosis in the budding yeast S. cerevisiae. *Cell* 65(1):145–161.
56. Fishbein JD, Dobrowsky RT, Bielawska A, Garrett S, Hannun YA (1993) Ceramide-mediated growth inhibition and CAPP are conserved in Saccharomyces cerevisiae. *J Biol Chem* 268(13):9255–9261.
57. Nickels JT, Broach JR (1996) A ceramide-activated protein phosphatase mediates ceramide-induced G1 arrest of Saccharomyces cerevisiae. *Genes Dev* 10(4):382–394.
58. McCourt P, Gallo-Ebert C, Gonghong Y, Jiang Y, Nickels JT, Jr (2013) PP2A(Cdc55) regulates G1 cyclin stability. *Cell Cycle* 12(8):1201–1210.
59. Matmati N, et al. (2013) Identification of C18:1-phytoceramide as the candidate lipid mediator for hydroxyurea resistance in yeast. *J Biol Chem* 288(24):17272–17284.
60. Anastasia SD, et al. (2012) A link between mitotic entry and membrane growth suggests a novel model for cell size control. *J Cell Biol* 197(1):89–104.
61. McCusker D, Kellogg DR (2012) Plasma membrane growth during the cell cycle: Unsolved mysteries and recent progress. *Curr Opin Cell Biol* 24(6):845–851.
62. McCusker D, Royou A, Velours C, Kellogg D (2012) Cdk1-dependent control of membrane-trafficking dynamics. *Mol Biol Cell* 23(17):3336–3347.
63. Allen C, et al. (2006) Isolation of quiescent and nonquiescent cells from yeast stationary-phase cultures. *J Cell Biol* 174(1):89–100.
64. Gray JV, et al. (2004) "Sleeping beauty": Quiescence in Saccharomyces cerevisiae. *Microbiol Mol Biol Rev* 68(2):187–206.
65. Pardee AB (1989) G1 events and regulation of cell proliferation. *Science* 246(4930):603–608.
66. Piñon R (1978) Folded chromosomes in non-cycling yeast cells: Evidence for a characteristic g0 form. *Chromosoma* 67(3):263–274.
67. Pringle JR, Hartwell LH (1981) Saccharomyces cerevisiae cell cycle. *Molecular Biology of the Yeast Saccharomyces*, eds Broach J, Strathern J, Jones E (Cold Spring Harbor Lab Press, Cold Spring Harbor, NY).
68. Drebot MA, Johnston GC, Singer RA (1987) A yeast mutant conditionally defective only for reentry into the mitotic cell cycle from stationary phase. *Proc Natl Acad Sci USA* 84(22):7948–7952.
69. Martinez MJ, et al. (2004) Genomic analysis of stationary-phase and exit in Saccharomyces cerevisiae: Gene expression and identification of novel essential genes. *Mol Biol Cell* 15(12):5295–5305.
70. Laporte D, et al. (2011) Metabolic status rather than cell cycle signals control quiescence entry and exit. *J Cell Biol* 192(6):949–957.
71. Zakrajšek T, Raspor P, Jamnik P (2011) Saccharomyces cerevisiae in the stationary phase as a model organism—Characterization at cellular and proteome level. *J Proteomics* 74(12):2837–2845.
72. McNulty JJ, Lew DJ (2005) Swe1p responds to cytoskeletal perturbation, not bud size, in S. cerevisiae. *Curr Biol* 15(24):2190–2198.
73. Wach A, Brachat A, Alberti-Segui C, Rebischung C, Philippsen P (1997) Heterologous HIS3 marker and GFP reporter modules for PCR-targeting in Saccharomyces cerevisiae. *Yeast* 13(11):1065–1075.
74. Villa-García MJ, et al. (2011) Genome-wide screen for inositol auxotrophy in Saccharomyces cerevisiae implicates lipid metabolism in stress response signaling. *Mol Genet Genomics* 285(2):125–149.
75. Baerends RJ, et al. (2000) A stretch of positively charged amino acids at the N terminus of Hansenula polymorpha Pex3p is involved in incorporation of the protein into the peroxisomal membrane. *J Biol Chem* 275(14):9986–9995.
76. Lianga N, et al. (2013) A Wee1 checkpoint inhibits anaphase onset. *J Cell Biol* 201(6):843–862.

77. Rudner AD, Murray AW (2000) Phosphorylation by Cdc28 activates the Cdc20-dependent activity of the anaphase-promoting complex. *J Cell Biol* 149(7):1377–1390.
78. Knittelfelder OL, Weberhofer BP, Eichmann TO, Kohlwein SD, Rechberger GN (2014) A versatile ultra-high performance LC-MS method for lipid profiling. *J Chromatogr B Analyt Technol Biomed Life Sci* 951-952:119–128.
79. Folch J, Lees M, Sloane Stanley GH (1957) A simple method for the isolation and purification of total lipides from animal tissues. *J Biol Chem* 226(1):497–509.
80. Hartler J, Tharakan R, Köfeler HC, Graham DR, Thallinger GG (2013) Bioinformatics tools and challenges in structural analysis of lipidomics MS/MS data. *Brief Bioinform* 14(3):375–390.